Irrig Sci (2004) 23: 123–131
DOI 10.1007/s00271-004-0100-3

ORIGINAL PAPER

R. Fernández-Gómez · L. Mateos · J. V. Giráldez

Furrow irrigation erosion and management

Received: 30 June 2003 / Accepted: 7 July 2004 / Published online: 18 August 2004

Abstract Irrigation-induced furrow erosion reduces topsoil depth and pollutes surface waters. A variety of interacting factors, including inflow rate, slope and soil type, are known to affect furrow erosion. Data are inadequate to understand the furrow erosion process sufficiently well to recommend irrigation practices that maintain high levels of water quality and conserve soil. We performed furrow erosion field studies on two soils (a loamy textured alluvial soil and a clay loam cracking soil) with slopes ranging from 0.3 to 0.8%. Three inflow rates per furrow were applied in each of three irrigations. We found net rates of soil loss in the upper part of the furrow that were up to six times higher than the average net rate for the whole furrow. The soil loss was related to the inflow rate by power functions. High inflow rates on furrows with slopes greater than 0.3% caused unsustainable soil losses. However, at least in the loamy textured soil, it is possible to maintain high irrigation uniformity and application efficiency (within the range 80–85%), while keeping soil losses within a sustainable limit. An analysis of the sediment load data made in the frame of a simple conceptual model helped to explain the dynamics of the furrow erosion process and to establish the basis for modeling furrow erosion.

Communicated by A. Kassam

R. Fernández-Gómez
E.P. para el Desarrollo Agrario y Pesquero de Andalucía SA,
Alameda del Obispo s/n, Córdoba, Spain

L. Mateos (✉)
Instituto de Agricultura Sostenible, CSIC,
Apdo 4084, 14080 Córdoba, Spain
E-mail: ag1mainl@uco.es
Fax: +34-957-499252

J. V. Giráldez
Dpto de Agronomía, Universidad de Córdoba,
Avda Menéndez Pidal s/n, Córdoba, Spain

Introduction

Soil erosion is one of the most serious agricultural problems because it reduces soil fertility and contaminates surface waters. Past erosion studies have concentrated on rainfed agriculture, although fields irrigated either by surface- or sprinkler-applied water may yield substantial amounts of sediments.

Koluvek et al. (1993) reviewed irrigation-induced soil erosion studies carried out over 50 years in the USA. They referred to a survey by the USDA Soil Conservation Service showing that 21% of the irrigated land in the USA is affected by soil erosion. All but one of the surveyed studies were based on furrow irrigation. The review concluded that annual erosion rates of 2–11 Mg ha^{-1} are often exceeded in silty textured soils with slopes greater than 1%. Much higher soil loss rates have been reported in experimental studies (e.g., Berg and Carter 1980; Trout 1996).

Furrow erosion surveys are not available in Spain. However, the writers have observed great variation of furrow slopes (from 0.1 to 2%) and flow rates (from 0.5 to 2 l s^{-1}), and frequent signs of furrow erosion in the irrigated fields of southern Spain.

In furrow irrigation, water is released at the head inflow end of the furrow. As water advances downstream, the flow cross-section is smaller towards the water front, due to infiltration along the submerged part of the furrow. The inflow rate must be high enough to ensure that the flow reaches the end of the furrow and the duration of the application must satisfy the crop water requirements. Therefore, at least in the upper part of the furrow, the power of the stream may be sufficient to detach soil particles and to transport them further downstream or even out of the field. As the flow rate decreases along the furrow, the reduction in the transport (and detaching) capacity results in the deposition of sediments.

Furrow irrigation erosion studies conducted in the 1940s and 1950s focused on empirical functions relating soil losses to variables such as inflow rate, slope, and

furrow length (Mech and Smith 1967). Such functions were required in order to design rational furrow irrigation systems. Little attention was paid to the mechanisms of the erosion process, or to its spatial and temporal variations. While surface water contamination depends only on the sediments exported out of the field, soil degradation depends also on the within-field redistribution of soil particles. Renewed interest in irrigation-induced erosion, arising from an awareness of the need for soil conservation, has prompted more detailed studies and new conceptual approaches. In one of these experimental studies, Trout (1996) compiled one of the most complete data sets related to the furrow erosion process in silt loam soils. In addition, the models of Trout and Neibling (1993) and Fernández-Gómez (1997) have improved our understanding of the physical processes involved.

The aim of the study reported here was to extend the field assessment of the impact of furrow irrigation management and design variables on soil losses and within-furrow soil redistribution.

Conceptual framework

Trout and Neibling (1993) adapted the simple conceptual model of soil erosion developed by Foster and Meyer (1972) to furrow erosion. This approach assumes steady-state conditions and that both detachment and transport of soil particles are driven by the flow shear stress. According to this model, soil detachment, E [$ML^{-2}\ T^{-1}$], in the furrow occurs when the shear stress, τ [$ML^{-1}\ T^{-2}$], at the bed exceeds a critical shear value for the soil, τ_c [$ML^{-1}\ T^{-2}$], and the sediment load, T [MT^{-1}], is less than the flow transport capacity, T_c [MT^{-1}]. If there is no sediment load, transport does not limit detachment, and E becomes the maximum erosion capacity of the flow, E_c [$ML^{-2}\ T^{-1}$]. Then, E_c may be approximated by a linear relation with the shear stress:

$$E_c = k(\tau - \tau_c) \tag{1}$$

where k [$L^{-1}\ T$] is a measure of soil erodibility. Otherwise T and E are related by:

$$E = E_c\left(1 - \frac{T}{T_c}\right) \tag{2}$$

where T_c can be expressed as a power function of τ in a similar way to that suggested by Foster and Meyer (1972) based of an earlier expression of Yalin (1963):

$$T_c = k_t \tau^b \tag{3}$$

where k_t and b are empirical coefficients.

The equation of sediment mass conservation is written as

$$\frac{dT}{dx} = E \tag{4}$$

with x [L] distance from the furrow head.

As Meyer and Wischmeier (1969) stated, the net erosion rate becomes zero at the point where the sediment load equals the transport capacity, and net deposition, D [$ML^{-2}\ T^{-1}$], begins:

$$D = -\frac{dT_c}{dx} \tag{5}$$

The above relationships were deployed by Trout and Neibling (1993) to model the spatial variation in transport capacity, sediment transport, erosion, and deposition as the flow rate diminishes from the furrow head. We used this simple model in this study to help in the interpretation of our field measurements.

Methods

Two sites, and soils (Table 1), were used for the experiments. The first site was located at the Alameda del Obispo Research Station, Córdoba, Spain, with a loamy textured alluvial soil, Typic Xerofluvent (Soil Survey Staff 1999). Experiments at the Alameda del Obispo site were performed in the summers of 1994 and 1995. The second experimental site was the Casavacas farm, near Seville, Spain, with a clay loam cracking soil, Typic Haploxerert (Soil Survey Staff 1999), with high cohesivity between aggregates. The experiments at the Casavacas site were performed during the summer of 1996.

At Alameda del Obispo there were two adjacent experimental plots, one with a uniform slope of 0.3% and the other with a uniform slope of 0.8%. The average slope of the Casavacas experimental plot was 0.5%, but it varied from 0.65% at the head (0–40 m from the head), through 0.48 in the middle part of the plot (40–80 m from the head), to 0.38% in the lower part (80–120 m from the head). The furrow lengths differed between years (180 m in 1994, 200 m in 1995, and 120 m in 1996). Furrow spacing was 0.75 m at the Alameda del Obispo site and 0.96 m at the Casavacas site.

After ripping to about 0.6 m depth and cultivating the top 0.15 m, the experimental plots were planted with

Table 1 Soil classification and texture (0–0.15 m) of the two experimental sites

Experimental site	Year	Soil classification	Soil texture			
			Sand (%)	Silt (%)	Clay (%)	Texture class
Alameda del Obispo	1994	Typic Xerofluvent	35.0	44.3	20.6	Loamy
	1995		32.6	45.6	21.8	
Casavacas	1996	Typic Haploxerert	27.3	26.6	46.1	Clay loam

sunflower in Alameda del Obispo and cotton in Casavacas. The plots were furrowed when the plants were tall enough, and three irrigations were applied during each of the three experimental years. The first irrigation of each year was applied to freshly tilled and furrowed soil; the second and third were applied without further tillage between the irrigations.

The experimental plots were subdivided in order to apply and evaluate the effects of different inflow rates. In 1995 and 1996, each subplot had five furrows, the outer two of which acted as borders, while the other three were controlled; thus each inflow rate treatment was repeated in three furrows. In 1994, the subplots had only three furrows, and only the central one was controlled. We preferred this experimental design to a randomized design because the advance rate of the water front in a furrow is affected by its inflow rate; thus the infiltration and flow velocity in a furrow is affected by the inflow rate of the neighboring furrows.

The flow rates applied at the head end of the furrows for each of the subplots in each year are given in Table 2. Water was applied through a gated pipe and the inflows were adjusted based on flow measurements with RBC flumes (Clemmens et al. 1984) installed at the head of the controlled furrows. The inflow to the border furrows was not measured, but was adjusted in order to obtain an advance velocity similar to that in the controlled furrows. Additional flumes were installed in 1994 at intermediate distances and at the tail of the controlled furrow of each subplot. These flumes altered the water and sediment flows, so in the following years they were not installed. However, a kinematic-wave furrow irrigation model was able to simulate satisfactorily the water flow along the furrows in 1994; thus in 1995 and 1996 the water flow along the furrows and at the tail of the furrows was not measured but simulated.

During the irrigations, the water advance time was measured at 20-m intervals along the furrows. Water samples were collected at stations in the central furrow (Alameda del Obispo, 1994) or the three controlled furrows (Alameda del Obispo, 1995, and Casavacas, 1996) of each subplot. The sampling stations were located at three (1994 and 1996) or four (1995) distances from the head end (Table 2). The samples were collected after 15, 30, 75, 135, 195, and 255 min of wetting time at each sampling station in 1994 and 1995, and after 15, 30, 60, 90, 120, 150, 180, and 210 min in 1996. The 250-ml samples were taken by suctioning very slowly at approximately half the depth of the flow with a 100-ml syringe. At the sampling locations, the furrows were covered with rubber sheets in order to avoid undesirable sediment extraction from the furrow bed. These sheets were flexible enough to adapt to the furrow shape and heavy enough to prevent them from being dragged with the flow. The sediment samples were oven-dried in order to determine the sediment weight for the sampled volume.

The furrow cross-sectional geometry was measured at each sampling station with a furrow profilometer before each irrigation and after the last irrigation of the three experimental years.

Sediment load [MT^{-1}] in the flowing water was determined at each sampling station and time by multiplying the simulated water flow rate [$L^3\ T^{-1}$] by the measured sediment concentration [ML^{-3}]. This procedure has been tested by Mateos and Giráldez (2003). who concluded that it is a valid method, although it must be remembered that it slightly underestimates the total load.

The net soil loss upstream of each sampling station was obtained by integrating over time the sediment load measured at different wetting times.

Results

Soil loss and runoff water pollution are the two main environmental effects associated with furrow erosion. The first of these effects, soil loss, has a non-uniform on-field distribution (Carter 1990). In our experiment, net rates of soil loss in the head end portions of the plots were up to six times greater than the average net rate for the whole furrow (Fig. 1). In order to standardize results, the data presented in Fig. 1 refer to soil losses that occurred up to the time when a depth of 50 mm had infiltrated at the furrow tail. Average soil losses of up to 40 Mg ha^{-1} per irrigation (the area unit refers to the field area, not to the area of the wetted surface) were measured in the upper quarter of the furrows on the loamy soil with the maximum furrow inflow rate (Fig. 1a). The average rate in this treatment decreased to 15 Mg ha^{-1} per irrigation in the upper half and to 7.7 Mg ha^{-1} per irrigation in the whole subplot. The reduction in net soil losses observed as the tail of the field was approached indicates that a significant amount of detached soil is deposited and retained in the tail-end portions of the furrows, and only a fraction of it is

Table 2 Inflow rates at the furrows of the subplots of the three experimental years

Site	Soil	Year	Crop	Slope (%)	Irrigation	Inflows (l s^{-1})	Furrow length (m)	Furrow spacing (m)	Sampling station (m from head end)
Alameda del Obispo	Typic Xerofluvent, Loamy	1994	Sunflower	0.8	1,2,3	2.3 1.8 1.25	180	0.75	60, 120, 180
		1995	Sunflower	0.8	1,2,3	1.8 1.2 0.8	200	0.75	50, 100, 150, 200
				0.3	1,2,3	1.8	200	0.75	50, 100, 150, 200
Casavacas	Typic Haploxerert, Clay loam	1996	Cotton	0.5	1	3.0 2.3 1.5	120	0.96	40, 80, 120
				0.5	2,3	2.4 1.8 1.0	120	0.96	40, 80, 120

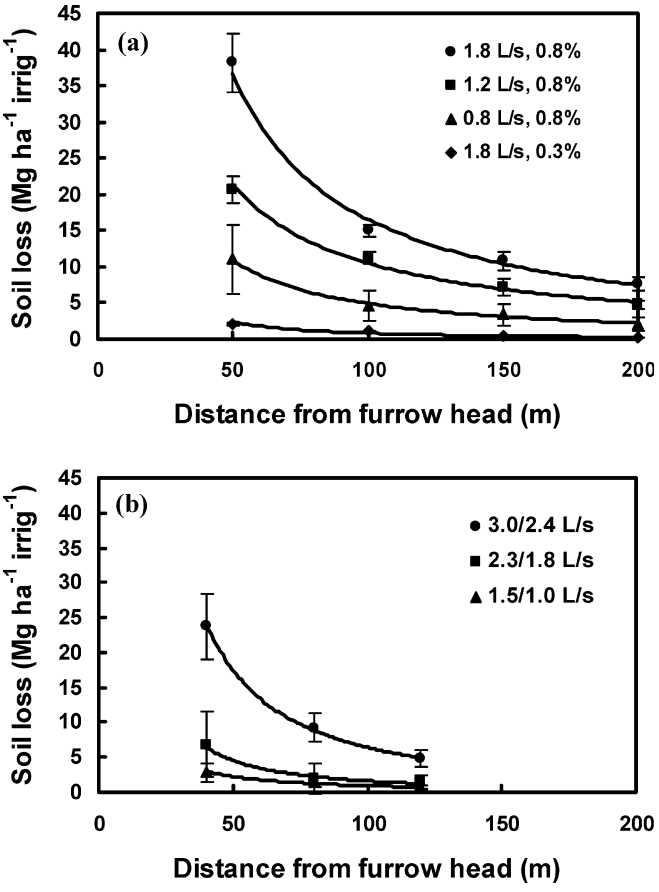

Fig. 1 Net soil loss as a function of distance from the furrow head, inflow rate and furrow slope in **a** the loamy soil, 1995, and **b** the clay loam soil. The *bars* indicate ± half the standard deviation of the three controlled furrows

exported out of the field. Trout (1996) observed similar on-field distributions on two silty loam soils. He divided the experimental furrows into four reaches. The amount of sediment transported out of the upper quarter was 6–20 times greater than the amount discharging from the lower end of the furrows.

The clay loam soil in our study showed similar behavior, but net soil loss rates were much lower than those for the loamy soil (Fig. 1b). Note that as well as differing in soil texture and structure, the slope at the Casavacas site was less than at the steeper plot at the Alameda del Obispo site, and it decreased considerably towards the tail end of the furrows.

The effect of the slope is evident if we compare the curves for the inflow rate of 1.8 l s^{-1} obtained for the slopes of 0.3 and 0.8% in the loamy soil (Fig. 1a). The amount of soil passing the upper sampling station was equivalent to 2.13 Mg ha^{-1} per irrigation in the 0.3% subplot, while it exceeded 35 Mg ha^{-1} per irrigation in the 0.8% subplot with an equivalent inflow rate. Similarly, the sediment exported out of the field through the lower end of the furrows was 0.27 Mg ha^{-1} per irrigation in the 0.3% subplot, and 7.63 Mg ha^{-1} per irrigation in the equivalent 0.8% subplot.

In order to assess the damage caused by the irrigations to the soil, the sediment losses should be quantified for the upper part of the field, where erosion is most severe, and they should be compared to losses that result from alternative irrigation regimes. For this purpose, we evaluated the effect of the inflow rate, the main variable of furrow irrigation management. The circles in Fig. 2 show the soil losses that occurred in the upper part of the furrows up to the time when 50 mm of water have infiltrated at the furrow tail, as functions of the inflow rate. The soil loss–inflow rate relationship was almost linear in the loamy soil (Fig. 2a) and followed a power function (with exponent 2.6) in the clay loam soil (Fig. 2b). Therefore, although the erosion rates in the clay loam soil were lower than in the loamy soil, the former was more sensitive to increments in the inflow rate.

The whole-field net soil loss and the effect of the inflow rate on pollution by the run-off water is shown by the lower end measurements (squares in Fig. 2). These parameters were related by power functions in both soils, with exponents of 1.5 and 2.4 in the loamy and clay

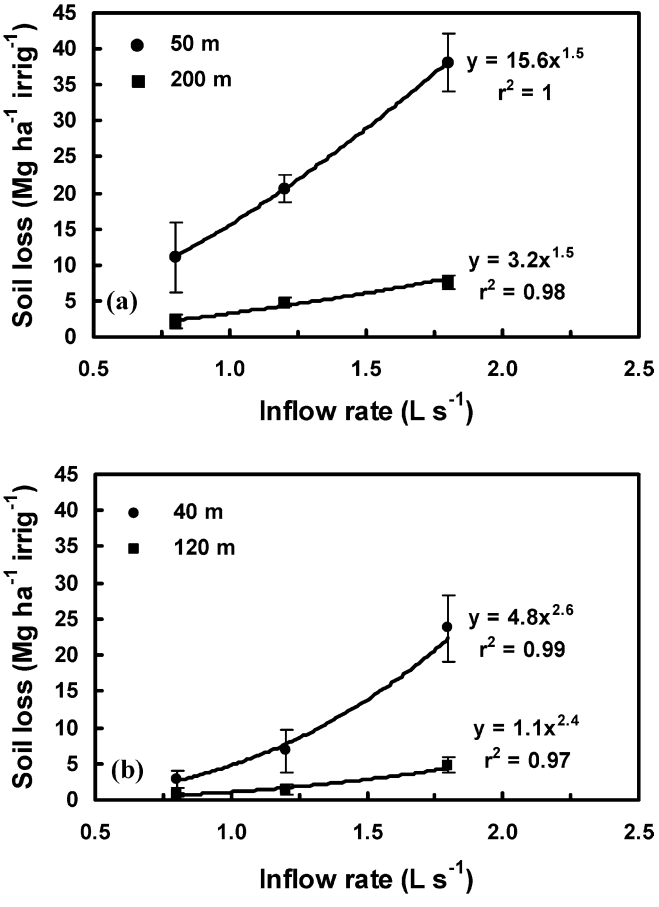

Fig. 2 Net soil loss in the upper part of the plot and the whole plot as a function of the inflow rate in **a** the loamy soil, 1995, and **b** the clay loam soil. The *bars* indicate ± half the standard deviation of the three controlled furrows. In the equations, y is soil loss (Mg ha^{-1} per irrigation) and x is inflow rate (l s^{-1})

loam soils, respectively. As also mentioned for the upper part of the field, the soil losses through the tail of the field in the loamy soil were less sensitive to increments in inflow rate than those in the clay loam soil. However, it should be borne in mind that the furrow slopes and lengths also differed between the two sites.

The soil loss tolerance, defined as the maximum amount of erosion at which the quality of a soil as a medium for plant growth can be maintained, can be estimated for our experimental sites using the USDA Natural Resources Conservation Service (2003), criteria as about 12 Mg ha^{-1} $year^{-1}$. Assuming irrigation as the main cause of soil loss and assuming the requirement of eight 50-mm-depth irrigations per year, the soil loss tolerance per irrigation event would be about 1.5 Mg ha^{-1} per irrigation. For whole-furrow length and irrigation event, this tolerance was exceeded in all the inflow treatments in the 0.8% slope plot on the loamy soil and in the highest inflow treatment on the clay loam soil. The soil loss for the whole furrow length in the 0.3% slope plot on the loamy soil and on the clay loam soil with the two lower inflow treatments was less than the tolerance. However, the soil loss in the head end portion of the furrows was always greater than the soil loss tolerance.

The water management regime in the trials was not designed to provide high irrigation efficiency, but to investigate furrow erosion dynamics. The irrigation performance was variable due to the wide range of inflow rates, furrow slopes and lengths, water application times, and soil infiltration characteristics. Often the irrigations produced high levels of run-off and resulted in low application efficiency. However, the range of application efficiency (E_a, defined as the amount of water stored in the root zone divided by the amount of water applied) and distribution uniformity (DU, defined as the ratio between the average infiltrated depth in the lower quarter of the furrow and the average infiltrated depth) allowed examination of the relationship between irrigation performance and soil losses. Uniformity normally increases with the velocity of the water advance and the time during which water is flowing out the tail end of the furrows. Therefore, DU increased in our trials as the inflow rate, slope, and duration of irrigation increased—factors that also tended to increase the soil losses (Fig. 3). In contrast, high application efficiency in our trials implied low run-off, which was associated with low inflow rates and/or short irrigation times. Therefore, the lower the value of E_a, the higher were the soil losses. However, in the loamy soil, it was possible to set inflow rates and slopes that gave DU and E_a values within the range of 80–85% with acceptable soil losses (Fig. 3a). These results were produced from a varied but limited set of slopes, inflow rates, irrigation times, and soil conditions; thus the validity of the conclusions is restricted to the range of the data available. However, the irrigation performance–soil loss relationship for the clay loam soil (Fig. 3b) showed a pattern similar to that of the loamy soil, although with less soil loss. Unfortunately, we did not produce data in

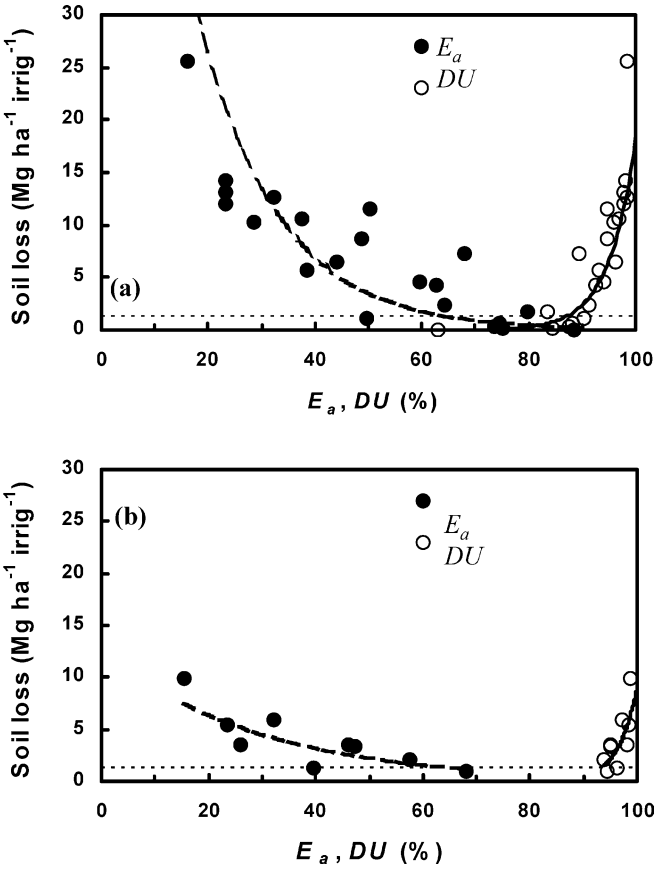

Fig. 3 Net soil loss at the tail end as a function of distribution uniformity (DU) and application efficiency (E_a) in **a** the loamy soil, in 1994 and 1995, and **b** the clay loam soil. The *horizontal dashed line* at 1.5 Mg ha^{-1} per irrigation represents the soil loss tolerance

the E_a and DU 80–85% interval, and thus we cannot assert that an optimal combination of DU, E_a and soil loss can be achieved with the soil type and furrow design in the clay loam soil.

The soil loss data could be used to set furrow irrigation design parameters, management criteria, and maximum flow rates that do not cause erosion. Hart et al. (1983) recommended that flow velocities should not exceed 0.15 m s^{-1} in "erosive soils" and 0.18 m s^{-1} in "less erosive soils". Walker and Skogerboe (1987) chose similar criteria but set the velocity thresholds at 0.13 m s^{-1} for "erosive silty soils" and 0.21 m s^{-1} for "more stable clay and sandy soils". Classifying the loamy soil as an "erosive soil" and the clay loam soil as a "less erosive" or "more stable" soil, only two of the treatments, both applied to the loamy soil, tested in our study would come close to satisfying such non-erosive criteria. These are the treatments applied to the 0.3% slope subplot (with flow velocity estimated from inflow rate and wetted section measurements at the inflow point of 0.15 m s^{-1}) and the 0.8 l s^{-1} inflow treatment applied to the 0.8% slope subplot (with estimated flow velocity of 0.17 m s^{-1}). It is noteworthy that, even in these two cases, the losses differed by an order of magnitude (0.27 and 2.17 Mg ha^{-1} per irrigation, respectively).

If, instead of the maximum velocity criteria, we use the slope–inflow relationship that Hamad and Stringham (1978) modified to separate the non-erosive and erosive regions in the slope–inflow plane (Fig. 4), we then find that all the treatments applied to the loamy soil, including the treatment on the 0.3% slope subplot, would be in the erosive region for a medium-textured soil. For the clay loam soil, only the lower inflow (with soil loss of 0.69 Mg ha^{-1} per irrigation) would fall into the non-erosion region if we assume that our soil is in the group of moderately-textured soils. Therefore, the non-erosion limit seems conservative but inconsistent, likely due to the simplicity of the models underlying the rules used to fix that limit.

Discussion

Sediment load may be limited either by erodible soil (supply) or by the transport capacity of the flow. Along a furrow, supply limitation is more likely to occur at the head, where the flow rate and shear are greater, and transport limitation at the tail, where flow rates are low.

We can discern how the soil type, inflow, and slope affected the erosion process in our experiments by observing the variation in sediment load at different distances from the furrow heads, and by using the above conceptual approach. First of all, for the highest flow rate, the measured load tended to decrease slightly with time at the head end (symbols in Fig. 5). Trout (1996) also observed that sediment concentration at a certain furrow location decreased continuously during a monitored irrigation, even though the flow rate approached a steady-state value within an hour of flow initiation at a location. He also mentioned several phenomena that may have changed the erodibility during the irrigation.

Our data can be used to calibrate k in Eq. 1 if we assume that deposition is negligible in the upper furrow reaches, that detachment occurs evenly along those reaches, and that the coefficients of the transport capacity function in Eq. 2 can be obtained by fitting the curve enveloping all the (T,τ) data points by eye (Fig. 6). Accepting these three premises and rearranging Eqs. 1 and 2, we obtain

$$E_c = \frac{E}{1-\frac{T}{T_c}} = k(\tau - \tau_c) \tag{6}$$

Erosion, E, transport, T, and transport capacity, T_c, were obtained from field measurements. Shear, τ, can be calculated using the kinematic-wave model. Thus k and τ_c can be estimated by regression analysis as the slope and the intercept divided by k, respectively (Table 3). Then, plotting the obtained k values against wetting time, a decrease in erodibility is observed in all the experiments (Fig. 7), confirming previous observations (e.g., Kabir and King 1981; Nearing et al. 1988) and

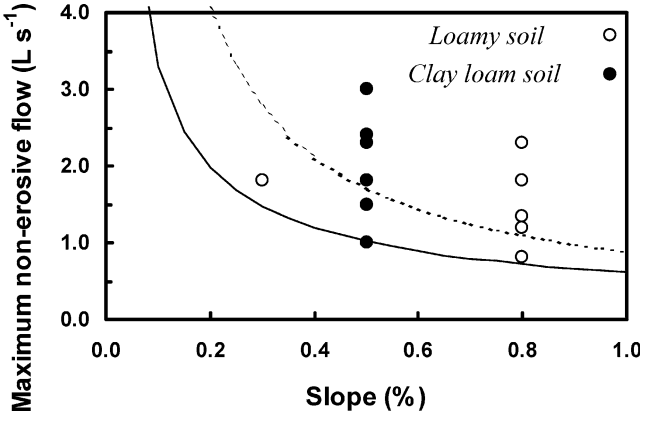

Fig. 4 Delineation of the non-erosive flow region (*below the lines*) and the erosive flow region (*above the lines*) as functions of the slope in medium-textured and moderately-textured soils, according to Hamad and Stringham (1978), compared with the inflow rates and slopes in the loamy soil and the clay loam soil

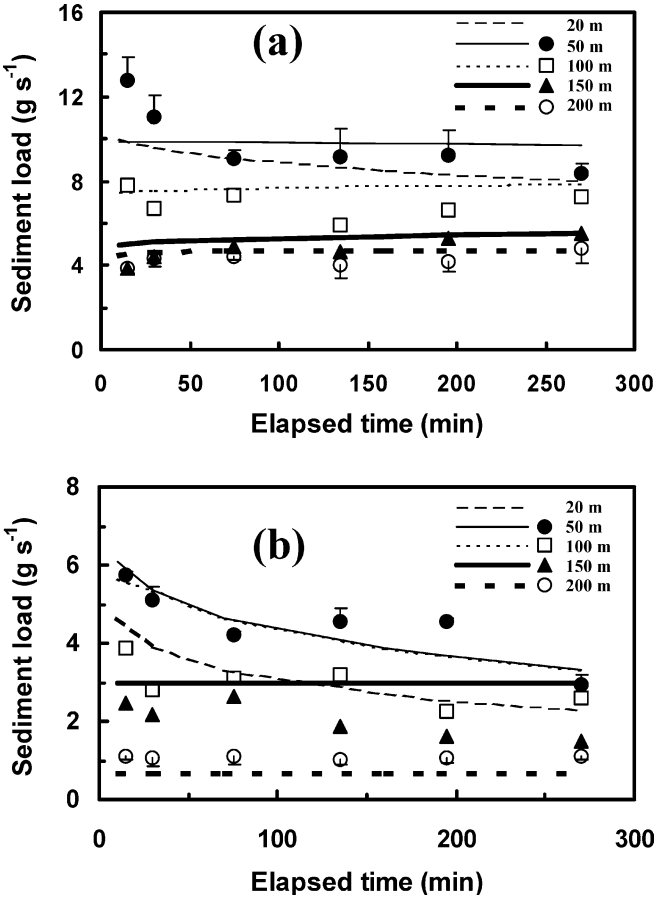

Fig. 5 Sediment load in two representative cases at various elapsed times and distances from the furrow head on the loamy soil, 1995, **a** 1st irrigation, inflow rate 1.8 l s^{-1} and slope 0.8%, and **b** 2nd irrigation, inflow rate 1.2 l s^{-1} and slope 0.8%, both in 1995. The *bars* indicate plus (50 m) or minus (200 m) half the standard deviation of the three controlled furrows (for clarity, the error bar has been indicated at only two of the four measuring distances). The *lines* represent the variation in sediment load generated by simulating successive states using Trout's model (1996)

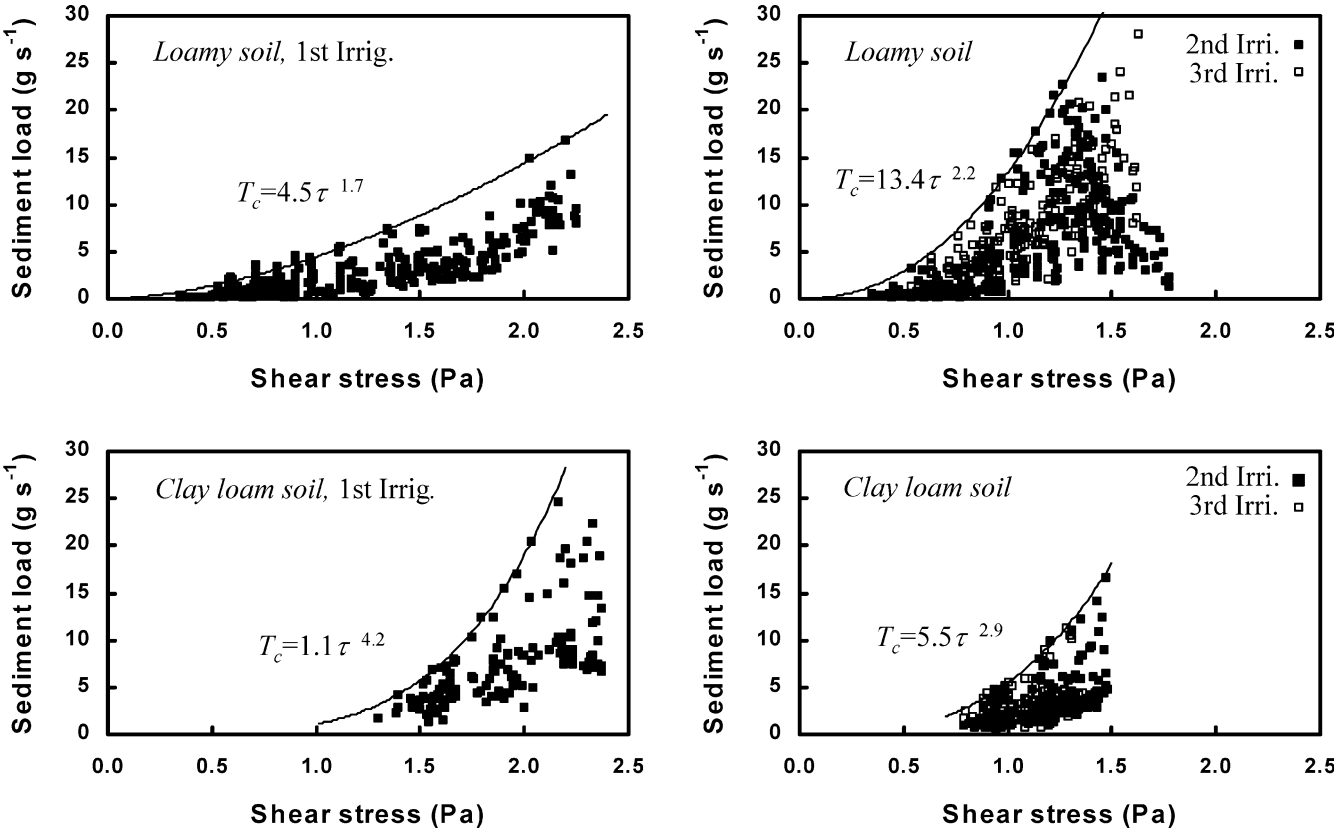

Fig. 6 Sediment load and adjusted transport capacity (T_c) for the sediment measurements for the three irrigations and each of the three experimental years

explaining the slight variation with time of the measured sediment load (Fig. 5). As can also be seen in Table 3, the values of τ_c obtained with the same regression analysis did not show significant variations, thus it seems that the decrease with time of the sediment load may be accounted for by variations in k.

Some authors (e.g., Wilcock and Southard 1989) have attributed the change in erodibility to the development of an armored layer as a consequence of the removal of fine particles, which exposes coarse particles that trap other fine particles below them. This phenomenon was apparent in the field, where we observed the development of a clear interface characterized by a sealed bed surface in the upper part of the furrows (where the supply limitation was most obvious), while downstream (where transport limitation occurred according to the load data) the bed–water flow interface was much more diffuse.

The slight decrease in sediment load observed at the 50-m location in Fig. 5 is not considered in the steady-

Table 3 Erodibility (k) and critical shear stress (τ_c) calibrated using all the data from the different years, slopes, irrigations, inflow rates and sampling times for each of the two soils. r^2 is the regression coefficient of the least squares linear regression

Soil	Wetting time (min)	First irrigation			Second and third irrigations		
		k (s m^{-1})	τ_c (Pa)	r^2	k (s m^{-1})	τ_c (Pa)	r^2
Typic Xerofluvent	15	0.00129	0.896	0.83	0.00256	0.689	0.69
	30	0.00123	0.774	0.78	0.00207	0.758	0.73
	75	0.00064	0.781	0.76	0.00164	0.740	0.74
	135	0.00082	0.824	0.89	0.00138	0.753	0.65
	195	0.00081	0.808	0.87	0.00106	0.686	0.76
	255	0.00062	0.866	0.89	0.00099	0.777	0.76
Typic Chromoxerert	15	0.00544	1.502	0.95	0.00426	0.856	0.74
	30	0.00529	1.479	0.89	0.00291	0.788	0.64
	60	0.00217	1.419	0.70	0.00285	0.862	0.64
	90	0.00272	1.198	0.73	0.00125	0.808	0.64
	120	0.00154	1.363	0.80	0.00104	0.847	0.60
	150	0.00247	1.511	0.87	0.00102	0.804	0.69
	180	0.00245	1.329	0.42	0.00066	0.728	0.62
	210	0.00179	1.491	0.60	0.00064	0.754	0.69

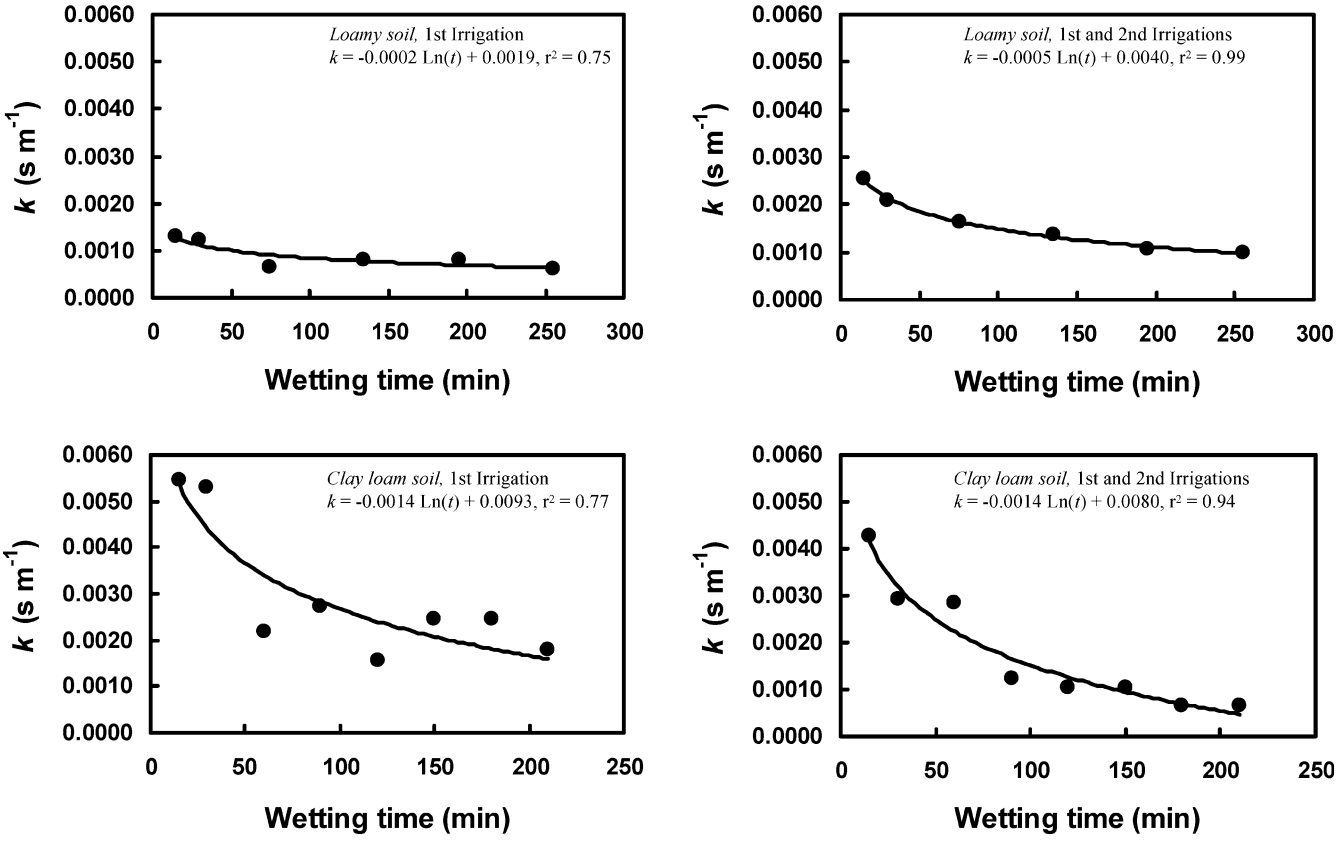

Fig. 7 Erodibility (k) as a function of wetting time derived from the sediment measurements taken during the three irrigations for each of the three experimental years

state conceptual framework. However, this variation in erodibility could be considered with the conceptual model by simulating a succession of steady-states in which k in Eq. 1 changes from one state to the next. The result of such an erosion process is represented by lines in Fig. 5. Close to the furrow head, the simulated sediment load decreases with time (distances 20 m in Fig. 5a and 20, 50, and 100 m in Fig. 5b), reflecting that erosion at these distances is supply-limited, and reproducing roughly the pattern of the field observations. Down along the furrow (distances 100, 150, and 200 m) the load does not change with time, but decreases with distance. These patterns indicate that erosion is transport-limited, and the limitation increases as the flow size decreases down the furrow.

We simulated sediment load also at 20 m from the furrow head, where measurements were not available. Sediment load at that distance was less than at 50 m and it decreased with time. This pattern would indicate that the closer to the furrow head, the more pronounced the supply limitation.

Similar speculations can be made for other cases, although the scatter of the data and the complexity of the process prevent reduction of the observed conditions to a simple model.

Conclusions

Furrow irrigation can cause excessive soil losses. This may lead to the degradation of the soil in the upper part of the field and pollution of the surface water receiving the tail water. For whole-furrow length and irrigation event, the soil loss tolerance was exceeded in all the inflow treatments in the 0.8% slope plot on the loamy soil and in the highest inflow treatment on the clay loam soil. The soil loss for the whole furrow length in the 0.3% slope plot on the loamy soil and on the clay loam soil with the two lower inflow treatments was less than the tolerance. However, the soil loss in the head-end portion of the furrows was always greater than the soil loss tolerance, indicating that periodical within-field soil redistribution is required to maintain the quality of the soil.

However, a finding of this study is that there is scope to manage irrigation in such a way as to achieve high irrigation uniformity and application efficiency, while keeping soil losses below a sustainable limit. This is certain for the loamy soil, but more combinations of inflow rates, furrow lengths, and slopes would be required to make the same claims for the clay loam soil. Additional experimental data, together with the development of simulation models, should assist in future to rationally establish the maximum non-erosive furrow inflow in relation to other irrigation variables. The simple conceptual approach used in this paper to interpret experimental results is a first approach that should

facilitate understanding of the furrow erosion process. More complex non-steady-state models would account for the dynamic processes observed in the field, but the suitability of each kind of model for the simulation of furrow erosion has yet to be demonstrated.

References

Berg RD, Carter DL (1980) Furrow erosion and sediment losses on irrigated cropland. J Soil Water Conserv 35:267–270

Carter DL (1990) Soil erosion on irrigated lands. In: Stewart BA, Nielsen DR (eds) Irrigation of agricultural crops. (Agronomy monograph 30) ASA-CSSA-SSSA, Madison, Wis., USA, pp 1143–1171

Clemmens AJ, Bos MG, Replogle JA (1984) Portable RBC flumes for furrow and earthen channels. Trans ASAE 27:1016–1026

Fernández-Gómez R (1997) La erosión del suelo en el riego por surcos. PhD thesis, University of Córdoba, Spain

Foster GR, Meyer LD (1972) A closed-form soil erosion equation for upland areas. In: Shen WH (ed) Sedimentation. Water Resources Publications, Fort Collins, Colo., USA

Hamad SN, Stringham GE (1978) Maximum nonerosive furrow irrigation stream size. J Irrig Drain Eng 104:275–281

Hart WE, Collins HG, Woodward G, Humphreys AS (1983) Design and operation of gravity or surface systems. In: Jensen ME (ed) Design and operation of farm irrigation systems. (ASAE monograph 3) American Society of Agricultural Engineers, St. Joseph, Mich., pp 501–580

Kabir J, King LG (1981) A numerical model of furrow irrigation sediment transport. ASAE paper 81-2529. Asae, St Joseph, Mich.

Koluvek PK, Tanji KK, Trout TJ (1993) Overview of soil erosion from irrigation. J Irrig Drain Eng 119:929–946

Mateos L, Giráldez JV (2003) Suspended load and bed load in irrigation furrows. Proceedings of the international symposium "25 years of assessment of erosion". Ghent, Belgium, 22–26 September 2003, pp 325–330

Mech SJ, Smith DD (1967) Water erosion under irrigation. In: Hagan RM, Haise HR, Edminster TW (eds) Irrigation of agricultural lands. Agronomy monograph 11, American Society of Agronomy, Madison, Wis., pp 950–963

Meyer LD, Wischmeier WH (1969) Mathematical simulation of the process of soil erosion by water. Trans ASAE 12:754–762

Nearing MA, West LT, Brown LC (1988) A consolidation model for estimating changes in rill erodibility. Trans ASAE 31:696–700

Soil Survey Staff (1999) Soil taxonomy: a basic system of soil classification for making and interpreting soil surveys, 2nd edn. (USDA agricultural handbook 436) USDA, Washington, D.C.

Trout TJ (1996) Furrow irrigation erosion and sedimentation: on-field distribution. Trans ASAE 39:1717–1723

Trout TJ, Neibling WH (1993) Erosion and sedimentation processes on irrigated fields. J Irrig Drain Eng 119:947–963

USDA Natural Resources Conservation Service (2003) National soil survey handbook. Available at http://soils.usda.gov/technical/handbook/

Walker WR, Skogerboe GV (1987) Surface irrigation: theory and practice. Prentice-Hall, Englewood Cliffs, N.J., USA

Wilcock PR, Southard JB (1989) Bed load transport of mixed size sediment: fractional transport rates, bed forms, and the development of a coarse bed surface layer. Water Resour Res 25:1629–1641

Yalin YS (1963) An expression for bed-load transportation. J Hydraul Divn ASCE 89:221–250